Quantum Probe and Design for a Chemical Compass with Magnetic Nanostructures

Jianming Cai
Institut für Quantenoptik und Quanteninformation der Österreichischen Akademie der Wissenschaften, Innsbruck, Austria

(Received 15 September 2010; revised manuscript received 10 November 2010; published 9 March 2011)

Magnetic fields as weak as Earth's may affect the outcome of certain photochemical reactions that go through a radical pair intermediate. When the reaction environment is anisotropic, this phenomenon can form the basis of a chemical compass and has been proposed as a mechanism for animal magnetoreception. Here, we demonstrate how to optimize the design of a chemical compass with a much better directional sensitivity simply by a gradient field, e.g., from a magnetic nanostructure. We propose an experimental test of these predictions, and suggest design principles for a hybrid metallic-organic chemical compass. In addition to the practical interest in designing a biomimetic weak magnetic field sensor, our result shows that gradient fields can serve as powerful tools to probe spin correlations in radical pair reactions.

DOI: 10.1103/PhysRevLett.106.100501 PACS numbers: 03.67.−a, 03.65.Yz, 82.30.−b

Introduction.—Recently there has been increasing interest in quantum biology, namely, investigating quantum effects in chemical and biological systems, e.g., light harvesting systems [1], avian compass [2–5] and olfactory sense [6]. The main motivation is to understand how quantum coherence (entanglement) may be exploited for the accomplishment of biological functions. As a key step towards this goal, it is desirable to find tools that can detect quantum effects under ambient conditions. The ultimate goal of practical interest in studying quantum biology is to learn from nature and design highly efficient devices that can mimic biological systems in order to complete important tasks, e.g., collecting solar energy and detecting weak magnetic field.

As an example of quantum biology, the radical pair mechanism is an intriguing hypothesis [7] to explain the ability of some species to respond to weak magnetic fields [8–10], e.g., birds [11–13], fruit flies [14], and plants [15]. A magnetochemical compass could find applications in remote magnetometry, in magnetic mapping of microscopic or topographically complex materials, and in imaging through scattering media [16]. It was demonstrated that a synthetic donor-bridge-acceptor compass composed of a linked carotenoid (C), porphyrin (P), and fullerene (F) [17] can work at low temperature (193 K). It is surprising that such a triad molecule is the only known example that has been experimentally demonstrated to be sensitive to the geomagnetic field (yet not at room temperature). It is currently not known how one might construct a biomimetic or synthetic chemical compass that functions at ambient temperature.

In this Letter, we approach the goals of studying quantum biology in the context of chemical compass by demonstrating that a suitably designed gradient field can significantly improve the performance of a model chemical compass (apart from increasing the intersystem crossing rate [18]), see Fig. 1. It also opens a possible route to probe spin correlations of radical pairs and thereby investigate the role of quantum effects in spin chemistry. The gradient field is strong at the location of one spin, and approximately zero at the other. Such a field can be created in the vicinity of a hard ferromagnetic nanostructure [18], by applying a spatially uniform bias field that cancels the field of the nanostructure in a small region of space. In essence, the strong gradient field at one spin can substitute for strong anisotropic hyperfine couplings required for a purely molecular compass. This geometry provides a more significant anisotropy and thereby shows much larger directional sensitivity than does the conventional compass mechanism based only on anisotropic hyperfine couplings. Without requiring extra nuclear spins, the present model can work merely with two electron spins and thereby much simplifies quantum simulations of a chemical compass. With more freedom to tune parameters in a better controllable environment, such kind of quantum simulations would be helpful to understand the recombination process of radical pairs, in particular, whether and how quantum measurement and Zeno effect take place [4,5].

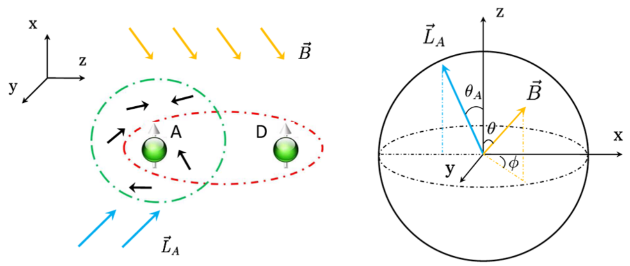

FIG. 1 (color online). Left: A radical pair, coupled with the surrounding nuclear spins (black arrows), in a weak magnetic field $\vec{B}$ to be measured (yellow [light gray] arrows) and a strong magnetic gradient $\vec{L}_A$ (blue [dark gray] arrows). Right: The directions of $\vec{B}$ and the gradient field at the location of the acceptor $\vec{L}_A$ depicted in the molecular coordinate frame.

Chemical compass mechanism.—Many chemical processes involve a radical pair intermediate, in which each radical has an unpaired electron coupled to an external magnetic field and a few nuclei via the Hamiltonian [19]

$$H = \sum_{k=A,D} H_k = -\gamma_e \sum_k \vec{B}_k \cdot \vec{S}_k + \sum_{k,j} \vec{S}_k \cdot \hat{\lambda}_{k_j} \cdot \vec{I}_{k_j} \qquad (1)$$

where $\gamma_e = -g_e \mu_B$ is the electron gyromagnetic ratio, $\hat{\lambda}_{k_j}$ denote the hyperfine coupling tensors and $\vec{S}_k$, $\vec{I}_{k_j}$ are the electron and nuclear spin operators, respectively. In our model, the magnetic field consists of two parts: $\vec{B}_k = \vec{B} + \vec{L}_k$, where the directional information about $\vec{B}$ is what one wants to infer from the radical pair reaction, and $\vec{L}_k$ is the local gradient field applied to each radical and is independent of $\vec{B}$. The spin relaxation and decoherence times resulting from the factors other than hyperfine interactions are assumed to be considerably longer than the radical pair lifetime [3,11], to maximize sensitivity to weak magnetic fields [20]. In many photochemical processes, the radical pair is created in a spin-correlated electronic singlet state $|\mathbb{S}\rangle = \frac{1}{\sqrt{2}}(|\uparrow\downarrow\rangle - |\downarrow\uparrow\rangle)$ within the time scale of picoseconds. The nuclear spins start at thermal equilibrium, which under ambient conditions leads to an approximate density matrix as $\rho_n(0) = \bigotimes_j \mathbb{I}_j / d_j$, where d_j is the dimension of the jth nuclear spin and $\mathbb{I}_j$ is the identity matrix. The Zeeman splitting from a magnetic field $\vec{B}$ as weak as the geomagnetic field is much smaller than the thermal energy at ambient temperature. Nonetheless, the field can influence the nonequilibrium electron spin dynamics and thereby determine the ratio of the chemical product from the singlet or triplet recombination as long as the thermalization time is longer than the reaction time.

In experiments, one may measure different quantities that are dependent on the weak magnetic field $\vec{B}$. Here we consider a simple first-order recombination reaction of the singlet radical pairs. We note that there is some controversy over how to describe the radical pair reactions (see, e.g., [4,5,21,22]). Nevertheless, the conventional phenomenological density matrix approach [19] works well in most cases, in particular, when the singlet and triplet recombination rates are the same (i.e. $k_S = k_T = k$) [23]. We adopt this method and calculate the singlet yield as $\Phi_S = \int_0^\infty f(t) P_S(t) dt$, where $f(t) = ke^{-kt}$ is the radical reencounter probability distribution, and $P_S(t) = \langle \mathbb{S} | \rho_s(t) | \mathbb{S} \rangle$ is the singlet fidelity for the electron spin state $\rho_s(t)$ at time t. The integration of Φ_S was performed following the method in [24,25].

Gradient enhancement of magnetic field sensitivity.—We start from an optimally designed hyperfine compass model, one radical has strong and anisotropic hyperfine interactions, and the other radical has no hyperfine couplings [20]. We arbitrarily choose to call the first radical the acceptor, A, and the second the donor, D, though nothing that follows depends on this designation. Ritz and coworkers proposed that the radical pair $\mathrm{FADH}^{\cdot}$-$\mathrm{O}_2^{\cdot -}$ meets this criterion, and they further speculated that this radical pair may be responsible for the magnetoreception of European robins [20], see also [26]. Without loss of the essential physics, we take the hyperfine couplings from $\mathrm{FADH}^{\cdot}$-$\mathrm{O}_2^{\cdot -}$ [27] for our calculations.

We define the molecular frame as the coordinate system, and the weak magnetic field $\vec{B}$ can be represented as $\vec{B} = B(\sin\theta\cos\phi, \sin\theta\sin\phi, \cos\theta)$. The gradient field induces different local fields on two radicals. We assume that the gradient field on the acceptor radical is $\vec{L}_A = L_A(\sin\theta_A, 0, \cos\theta_A)$ while $\vec{L}_D = 0$ for the donor radical. The strength of the weak magnetic field to be detected is the same as the geomagnetic field, i.e. $B = 0.46$ G. To demonstrate the basic idea, we first consider $\phi = 0$, and then generalize to arbitrary ϕ.

In Fig. 2(a), we plot the singlet yield as a function of the angle θ of the weak magnetic field $\vec{B}$. In the case of $L_A = 0$, the directionality comes only from hyperfine anisotropy. The gradient field clearly enhances the amplitude of the direction-dependent component of the magnetic field effect (MFE). To quantify the directional sensitivity, we use the magnetic visibility defined as $V = (\max\Phi_S - \min\Phi_S)/(\max\Phi_S + \min\Phi_S)$ [2]. As the gradient field becomes larger, the sensitivity will increase and approach a saturated best value. Figure 2(b) shows that for long radical pair lifetimes, the visibility with the gradient field $L_A = 40$ G is almost twice the visibility without the gradient field. Usually, the radical pair lifetime should be very long (microseconds) to maximize the effect of weak magnetic field [20], and hence performance, of the chemical compass [Fig. 2(b)]. This requirement places a severe constraint on the chemistry; in typical radical pair reactions the lifetime is less than 100 ns [19]. By increasing the overall magnitude of the visibility, gradient enhancement broadens the range of candidate reactions for a chemical compass.

Liquid crystal experiment.—In a uniaxially oriented sample, the MFE is averaged over all values of the

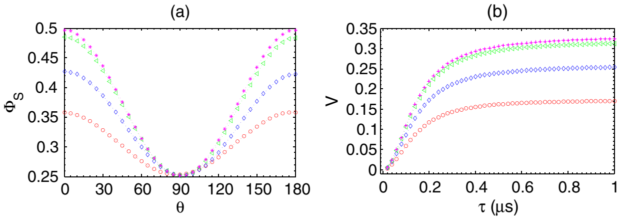

FIG. 2 (color online). Magnetic field sensitivity of a chemical compass enhanced by a gradient field. (a) Singlet yield Φ_S as a function of the angle θ of the weak magnetic field $\vec{B}$ ($B = 0.46$ G) with different gradient field strengths on the acceptor, i.e., $L_A = 0$ G (red [○]), 20 G (blue [◇]), 40 G (green [△]), 80 G (purple [*]), while $L_D = 0$. The recombination rate $k = 0.5\ \mu s^{-1}$. (b) Visibility V as a function of the radical pair lifetime $\tau = 1/k$. The direction of the gradient field $\vec{L}_A$ is set as $\theta_A = 0$. The same values of L_A are used as in (a).

angle ϕ. Such a sample is prepared by, for instance, freezing the molecules in a nematic liquid crystal in the presence of a strong magnetic field [17]. The ensemble-averaged MFE depends on θ only and is characterized by [17]

$$\langle \Phi_S(\theta) \rangle = \frac{1}{2\pi} \int_0^{2\pi} \Phi_S(\theta, \phi) d\phi. \tag{2}$$

It can be seen from Fig. 3(a) that the enhancement of the sensitivity can still be observed with the average signal $\langle \Phi_S(\theta) \rangle$ by choosing appropriate values of θ_A.

To induce the gradient field as above, one feasible way is to use magnetic nanostructures [18]. We model the nanocrystal as a uniformly magnetized sphere, in which case the external magnetic field is the same as that of a point dipole of magnetic moment $\mathbf{m}$ located at the center of the sphere [28]. We denote the position relative to the center of the sphere by the vector $\mathbf{r}$, and assume that both $\mathbf{r}$ and $\mathbf{m}$ lie along the z axis. The magnetic field at $\mathbf{r}$ is $\mathbf{B}(\mathbf{r}) = \frac{\mu_0 m}{2\pi r^3} \hat{\mathbf{r}}$, where $\mu_0 = 4\pi \times 10^{-7}\ \mathrm{N} \cdot \mathrm{A}^{-2}$ is the permeability of free space, the magnetic moment $m = M\varrho\Omega$ with M the specific magnetization, ρ is the material density, $\Omega = \frac{4}{3}\pi R^3$ is the volume of the particle and R is its radius. The parameters for the typical magnetic material $\mathrm{Fe_3O_4}$ are $M = 43\ \mathrm{A} \cdot \mathrm{m}^2 \cdot \mathrm{kg}^{-1}$, $\varrho = 5210\ \mathrm{kg} \cdot \mathrm{m}^{-3}$ [18]. For molecules with a separation r_{AD} between two radicals of a few nanometers [29], it is sufficient for a nanoparticle to induce a large local field imbalance (~ 10 G) on the donor and acceptor. For example, using a $\mathrm{Fe_3O_4}$ nanoparticle with $R = 15$ nm, it is possible to induce the local field difference to as large as $\simeq 40$ G between the position $r_A = 35$ nm and $r_D = r_A + r_{AD} = 38.5$ nm (assuming $r_{AD} = 3.5$ nm). By generating an additional homogenous field to compensate the field at the position r_D, we can effectively obtain the gradient field on the donor and acceptor as $L_A \simeq 40$ G and $L_D = 0$ G.

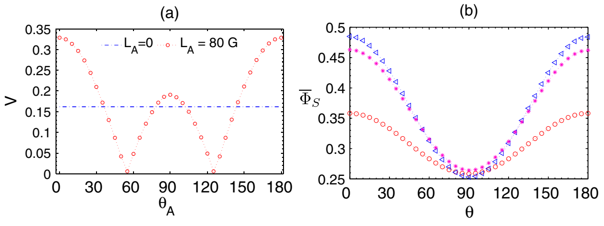

FIG. 3 (color online). (a) Visibility of the average singlet yield $\langle \Phi_S(\theta) \rangle$ as a function of the angle θ_A of the gradient field $L_A = 80$ G. The blue dash-dotted line represents the visibility without the gradient field. (b) Ensemble average of the singlet yield $\bar{\Phi}_S(\theta)$ in Eq. (3) from a Monte Carlo simulation of 2×10^4 samples as a function of the angle θ of the weak field $\vec{B}$. The gradient field is $L_A = 40$ G with $\theta_A = 0$ (purple [*]), while $L_D = 0$. For comparison, we plot the singlet yield with no gradient field (red [○]), and the one with the gradient field $L_A = 40$ G ($\theta_A = 0$) without fluctuations (blue [△]). The radical pair lifetime is 2 μs and $B = 0.46$ G.

To see whether the effect of the gradient field shown above can manifest with experimental imperfections, we take into account the fluctuations of $\vec{L}_A$ and $\vec{L}_D$ by modeling the fluctuation as the three-dimensional Gaussian distribution $f(\mathbf{\Delta}_i) = \frac{1}{(2\pi\sigma_i^2)^{3/2}} \exp(-\frac{|\mathbf{\Delta}_i|^2}{2\sigma_i^2})$ $(i = A, D)$ with $\sigma_A = 2$ G and $\sigma_D = 0.1$ G. Therefore, the ensemble average of $\langle \Phi_s(\theta) \rangle$ in Eq. (2) is

$$\bar{\Phi}_S(\theta) = \int \langle \Phi_S(\theta) \rangle |_{\mathbf{\Delta}_A, \mathbf{\Delta}_D} f(\mathbf{\Delta}_A) f(\mathbf{\Delta}_D) d\mathbf{\Delta}_A d\mathbf{\Delta}_D \tag{3}$$

where $\langle \Phi_S(\theta) \rangle |_{\mathbf{\Delta}_A, \mathbf{\Delta}_D}$ is the average singlet yield when the local fields on the acceptor and donor molecules are $\vec{L}_A + \mathbf{\Delta}_A$, $\vec{L}_D + \mathbf{\Delta}_D$, respectively. We have used Monte Carlo simulations to calculate the above ensemble average in Eq. (3). In Fig. 3(b), we see that the enhancement from the gradient field can still be observed.

Probe spin correlations in a chemical compass.—Besides the significant enhancement of the directional sensitivity offered by gradient fields, we now examine how they can provide new insights into the quantum dynamics of radical pair reactions. For the present model chemical compass, if the gradient field on the acceptor $\vec{L}_A$ dominates over the hyperfine couplings and the weak magnetic field $\vec{B}$, the singlet yield can be written as [25]

$$\Phi_S(\vec{L}_A, \vec{B}) = \frac{1}{4} - \frac{1}{4} \langle \hat{A} \otimes \hat{V} \rangle \tag{4}$$

where the expectation value is calculated over the initial state, and $\hat{A} = |u_0\rangle\langle u_0| - |u_1\rangle\langle u_1|$ (with $\{|u_0\rangle, |u_1\rangle\}$ the eigenstates of $\vec{L}_A \cdot \vec{S}_A$), $\hat{V} = \langle U_D^\dagger \hat{A} U_D \rangle$ with $U_D = \exp(i\gamma_e t\vec{B} \cdot \vec{S}_D)$ and the average taken over time weighted by $f(t)$. By choosing $\vec{L}_A$ in the direction of $\hat{x}$, $\hat{y}$, and $\hat{z}$, the corresponding operator $\hat{A}$ will be $\hat{X}$, $\hat{Y}$, $\hat{Z}$, respectively (which are the Pauli operators). Moreover, for each $\hat{A}$, one can choose $\hat{B}$ also in the direction of $\hat{x}$, $\hat{y}$, and $\hat{z}$ such that the operators of $\hat{V}$ (as a linear combination of Pauli operators) are linear independent, see [25]. The singlet yields corresponding to these choices of $\hat{L}_A$ and $\hat{B}$ lead to nine independent equations, from which we can infer the spin correlations $\langle \hat{M} \otimes \hat{N} \rangle$ for the radical pair state, where $\hat{M}, \hat{N} = \hat{X}, \hat{Y}$ or $\hat{Z}$. With these correlations, one may check whether the radical pair state violates Bell inequalities [30], or obtain lower entanglement bounds of the radical pair state, see Ref. [31].

As an example, we show that gradient fields can distinguish the singlet and the classically correlated initial state $\rho_c = (|\uparrow\downarrow\rangle\langle\uparrow\downarrow| + |\downarrow\uparrow\rangle\langle\downarrow\uparrow|)/2$. For systems where the radical pair lifetime is much longer than the decoherence time, the conventional hyperfine-mediated MFE does not strongly depend on the initial states and thus cannot allow one to achieve this goal, see, e.g., [2]. If the gradient field is along the z axis, the singlet yields are quite similar for the singlet and the classically correlated state

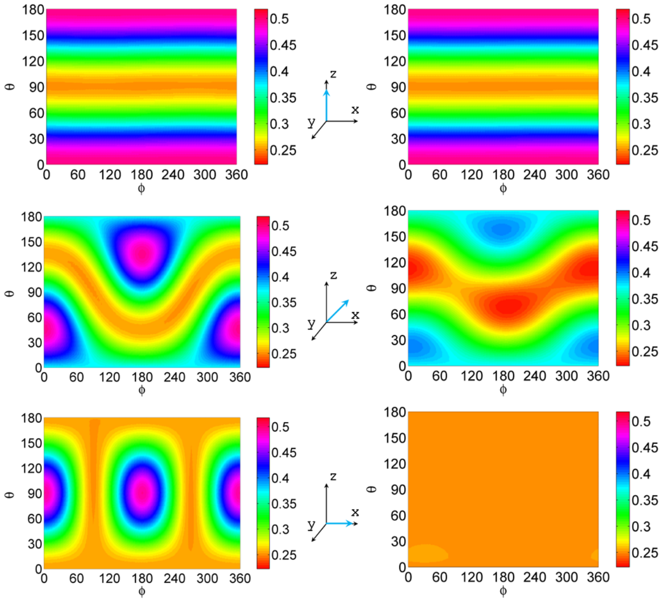

FIG. 4 (color online). The singlet yield Φ_S as a function of the angles (θ, ϕ) of the weak magnetic field $\vec{B}$ with $B = 0.46$ G. The gradient field on the acceptor is $L_A = 80$ G, on the donor it is $L_D = 0$. The angle of the gradient field θ_A with respect to the z axis is 0 (upper), $\frac{\pi}{4}$ (middle) and $\frac{\pi}{2}$ (lower). The radical pair lifetime is chosen as 2 μs.

[see Fig. 4 (upper)]. However, if we vary the direction of the gradient field $\vec{L}_A$, then the visibility for the singlet state will be much larger than for the classically correlated initial state [Fig. 4 (middle, lower)]. The difference originates from the essential boundary between classical and quantum correlation (entanglement). The large gradient field can be viewed as a measurement of the acceptor spin along $\vec{L}_A$: the singlet state demonstrates perfect anticorrelation of the spins for any direction of $\vec{L}_A$, while for the classically correlated state this is true only in a certain direction of $\vec{L}_A$ (i.e., the $\hat{z}$ direction).

Summary.—We have demonstrated that a gradient field can lead to a significant enhancement of the performance of a chemical compass. The gradient field also provides us with a powerful tool to investigate quantum dynamics of radical pair reactions in spin chemistry. These phenomena persist on addition of partial orientational averaging and of certain realistic magnetic noise. The effects predicted here may be detectable in a hybrid system compass composed of magnetic nanoparticles and radical pairs in an oriented liquid crystalline host. Our work offers a method to design a biologically inspired weak magnetic field sensor based on the radical pair mechanism with a high sensitivity that may work at room temperature.

We are in debt to Nan Yang and Adam Cohen for valuable suggestions and beneficial communications. We thank Kiminori Maeda, Gian Giacomo Guerreschi, and Otfried Gühne for helpful discussions, and Hans Briegel for continuous support in this work. The work is supported by FWF (SFB FoQuS).

[1] G. S. Engel *et al.*, Nature (London) **446**, 782 (2007); H. Lee *et al.*, Science **316**, 1462 (2007); E. Collini and G. D. Scholes, Science **323**, 369 (2009); M. Mohseni *et al.*, J. Chem. Phys. **129**, 174106 (2008); M. B. Plenio, S. F. Huelga, New J. Phys. **10**, 113019 (2008); F. Caruso, A. W. Chin, A. Datta, S. F. Huelga, and M. B. Plenio, J. Chem. Phys. **131**, 105106 (2009); M. Sarovar, A. Ishizaki, G. R. Fleming, and K. B. Whaley, Nature Phys. **6**, 462 (2010).
[2] J.-M. Cai, G. G. Guerreschi, and H. J. Briegel, Phys. Rev. Lett. **104**, 220502 (2010).
[3] E. Gauger *et al.*, Phys. Rev. Lett. **106**, 040503 (2011).
[4] I. K. Kominis, Phys. Rev. E **80**, 056115 (2009).
[5] J. A. Jones, P. J. Hore, Chem. Phys. Lett. **488**, 90 (2010).
[6] L. Turin, J. Theor. Biol. **216**, 367 (2002); J. C. Brookes, F. Hartoutsiou, A. P. Horsfield, and A. M. Stoneham, Phys. Rev. Lett. **98**, 038101 (2007).
[7] K. Schulten, C. E. Swenberg, and A. Weller, Z. Phys. Chem. Neue Folge **111**, 1 (1978).
[8] R. Wiltschko and W. Wiltschko, BioEssays **28**, 157 (2006).
[9] S. Johnsen and K. J. Lohmann, Nat. Rev. Neurosci. **6**, 703 (2005).
[10] C. T. Rodgers and P. J. Hore, Proc. Natl. Acad. Sci. U.S.A. **106**, 353 (2009).
[11] T. Ritz, S. Adem, and K. Schulten, Biophys. J. **78**, 707 (2000).
[12] W. Wiltschko and R. Wiltschko, J. Exp. Biol. **204**, 3295 (2001).
[13] T. Ritz *et al.*, Nature (London) **429**, 177 (2004).
[14] R. J. Gegear, A. Casselman, S. Waddell, and S. M. Reppert, Nature (London) **454**, 1014 (2008); R. J. Gegear, L. E. Foley, A. Casselman, and S. M. Reppert, *ibid.* **463**, 804 (2010).
[15] M. AhmadP. Galland, T. Ritz, R. Wilschko, and W. Wilschko, Planta **225**, 615 (2006).
[16] N. Yang, Y. Tang, and A. E. Cohen, Nano Today **4**, 269 (2009).
[17] K. Maeda *et al.*, Nature (London) **453**, 387 (2008).
[18] A. E. Cohen, J. Phys. Chem. A **113**, 11 084 (2009).
[19] U. E. Steiner, T. Ulrich, Chem. Rev. **89**, 51 (1989).
[20] T. Ritz *et al.*, Biophys. J. **96**, 3451 (2009).
[21] K. L. Ivanov, M. V. Petrova, N. N. Lukzen, and K. Maeda, J. Phys. Chem. A **114**, 9447 (2010).
[22] A. I. Shushin, J. Chem. Phys. **133**, 044505 (2010).
[23] In this case, the singlet yields calculated from different approaches are expected to be very similar [4,5,21,22].
[24] B. Brocklehurst, J. Chem. Soc., Faraday Trans. 2 **72**, 1869 (1976).
[25] See supplemental material at http://link.aps.org/supplemental/10.1103/PhysRevLett.106.100501, and also J.-M. Cai, arXiv:1011.5495, for calculation details.
[26] I. A. Solov'yov, K. Schulten, Biophys. J. **96**, 4804 (2009).
[27] F. Cintolesi *et al.*, Chem. Phys. **294**, 385 (2003).
[28] D. J. Griffiths, *Introduction to Electrodynamics* (Prentice Hall Inc., New Jersey, 1999), 3rd ed..
[29] M. Di Valentin, A. Bisol, G. Agostini, and D. Carbonera, J. Chem. Inf. Model. **45**, 1580 (2005).
[30] R. Horodecki, Phys. Lett. A. **210**, 223 (1996).
[31] K. M. R. Audenaert, M. B. Plenio, New J. Phys. **8**, 266 (2006).